Supporting Information

Fabrication of Pd/In_2O_3 Nanocatalysts Derived from MIL-68(In) Loaded with Molecular Metalloporphyrin (TCPP(Pd)) Towards CO_2 Hydrogenation to Methanol

Zhongjie Cai,[a] Meng Huang,[a] Jiajun Dai,[a] Guowu Zhan,[b] Fu-li Sun,[d] Gui-Lin Zhuang,[d] Yiyin Wang,[a] Pan Tian,[a] Bin Chen,[b] Shafqat Ullah,[a] Jiale Huang,[a]* and Qingbiao Li[a,b,c]*

[a] Department of Chemical and Biochemical Engineering, College of Chemistry and Chemical Engineering, Xiamen University, 422 Siming South Road, Xiamen, Fujian 361005, P. R. China

[b] College of Chemical Engineering, Integrated Nanocatalysts Institute (INCI), Huaqiao University, 668 Jimei Avenue, Xiamen, Fujian, 361021, P. R. China

[c] College of Food and Biology Engineering, Jimei University, 185 Yinjiang Road, Xiamen, Fujian 361021, P. R. China

[d] Institute of Industrial Catalysis, College of Chemical Engineering, Zhejiang University of Technology, Hangzhou, Zhejiang, 310032, P. R. China

**To whom correspondence should be addressed: gwzhan@hqu.edu.cn (Guowu Zhan) and cola@xmu.edu.cn (Jiale Huang)*

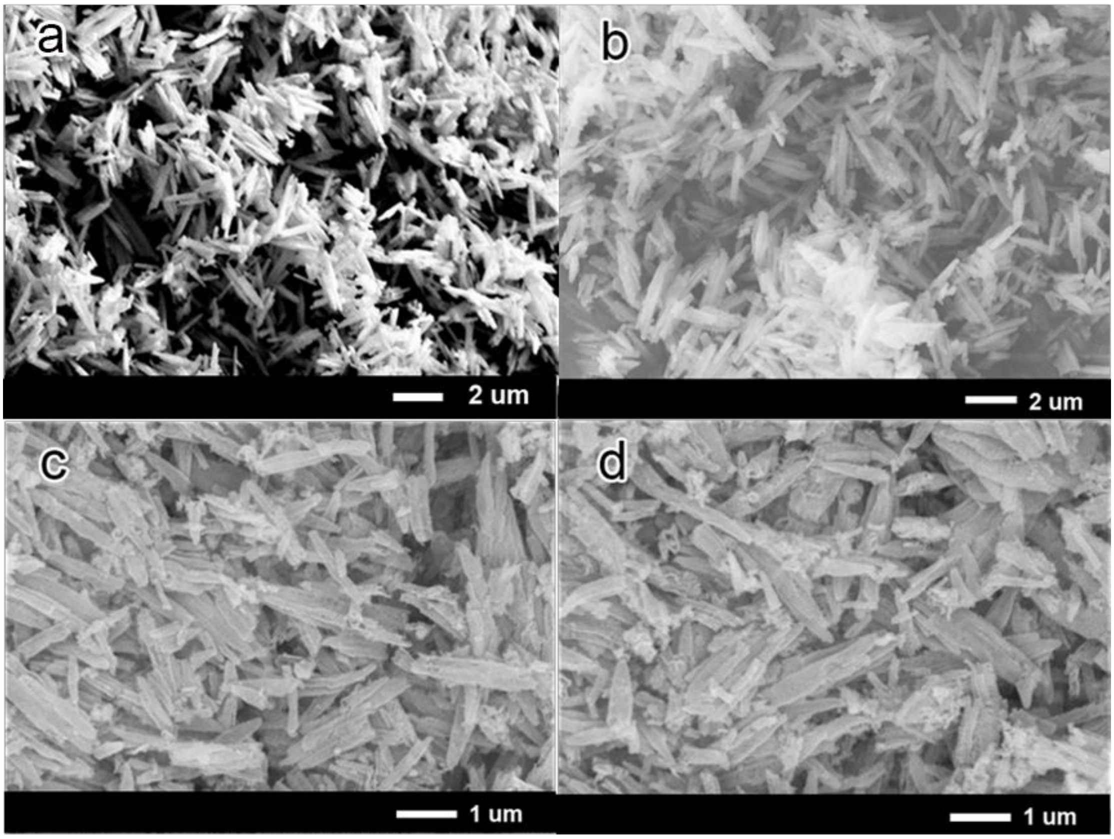

Figure S1. Representative SEM images of TCPP(Pd)@MIL-68(In) at TCPP(Pd) loading content of 1.9 wt% (a-b), and (c-d) derived Pd@In_2O_3 catalyst.

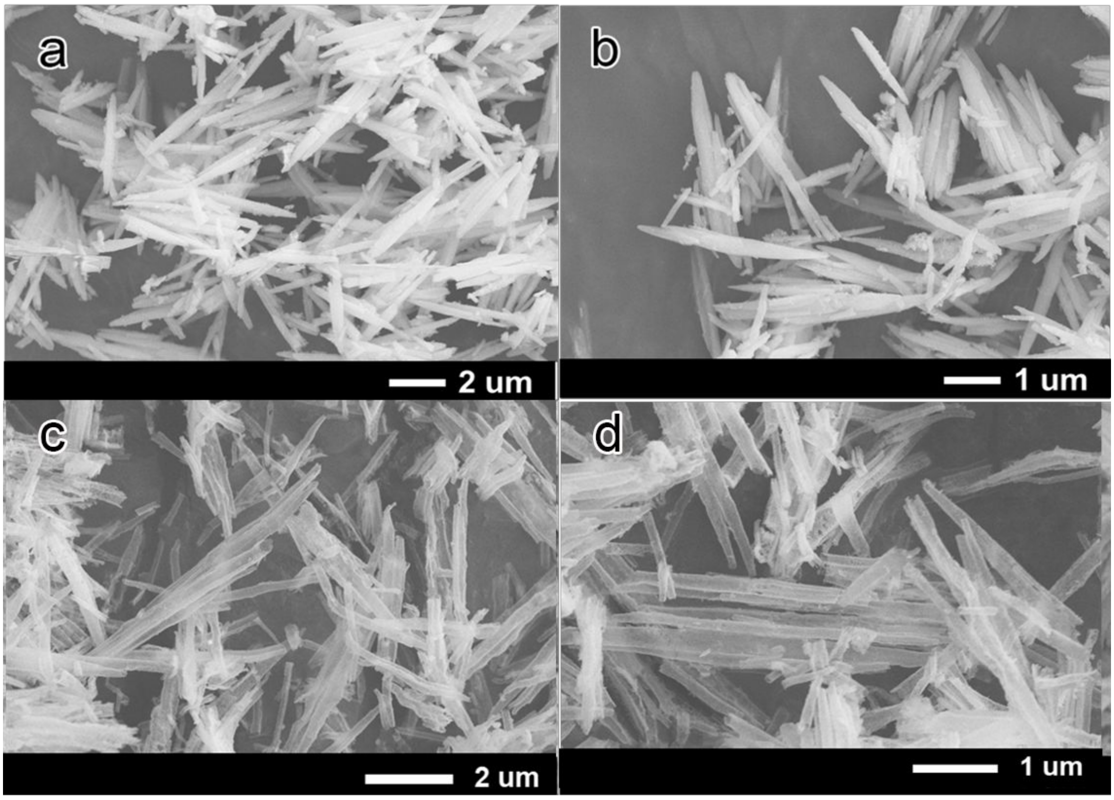

Figure S2. Representative SEM images of TCPP(Pd)@MIL-68(In) at TCPP(Pd) loading content of 3.8 wt% (a-b), and (c-d) derived Pd@In_2O_3 catalyst.

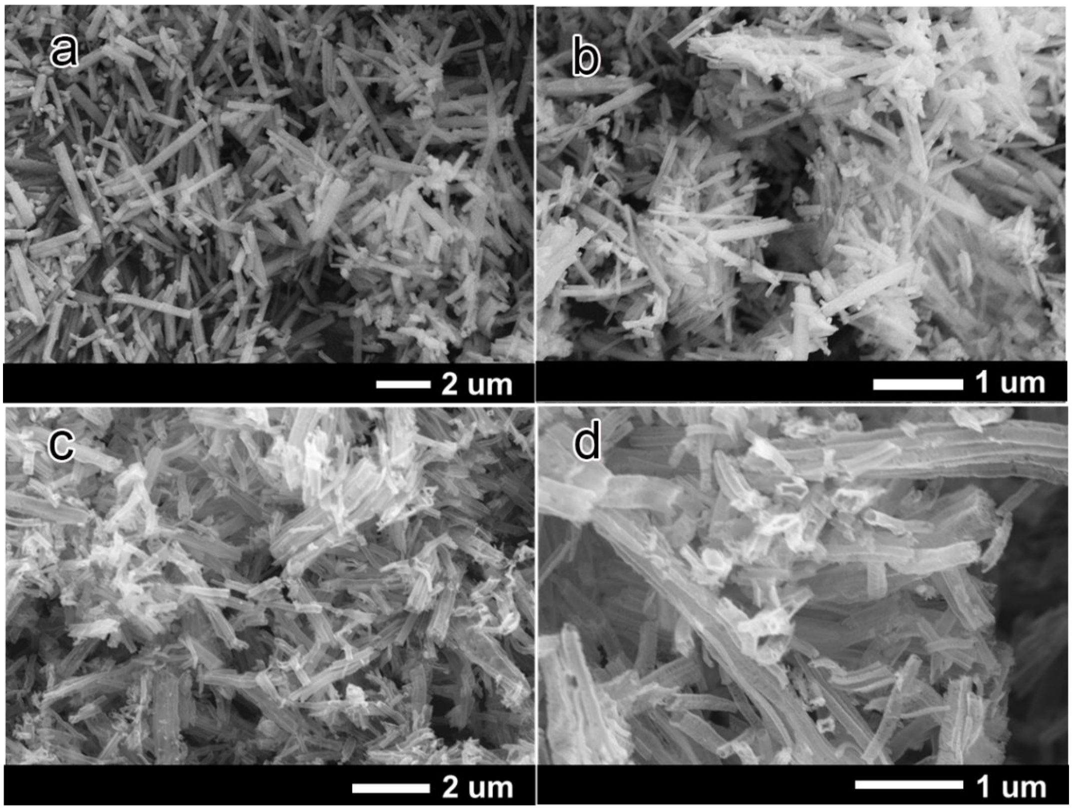

Figure S3. Representative SEM images of TCPP(Pd)@MIL-68(In) at TCPP(Pd) loading content of 4.7 wt% (a-b), and (c-d) the derived Pd@In_2O_3 catalyst.

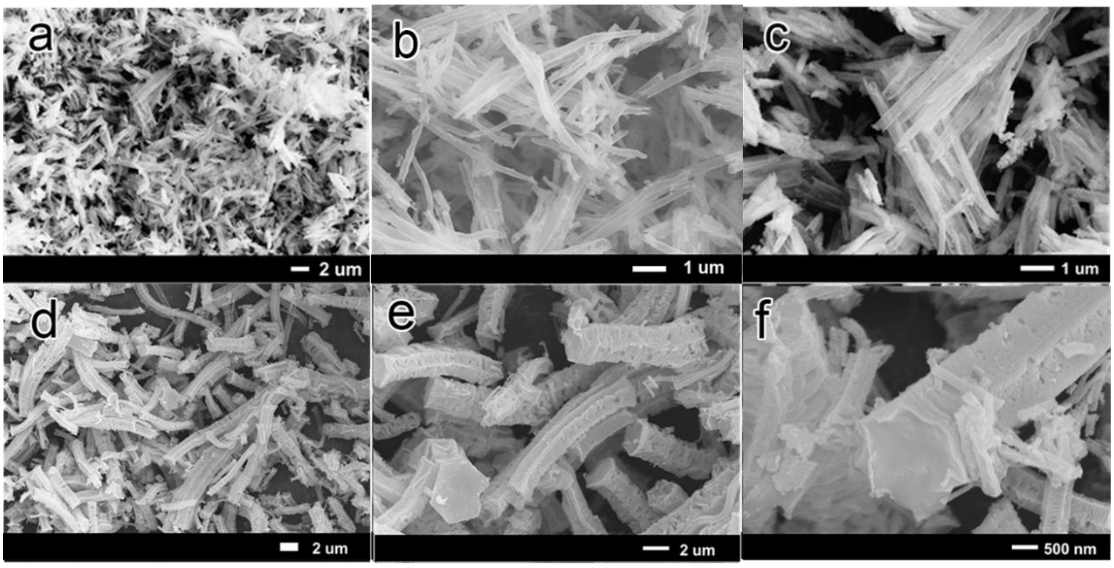

Figure S4. Representative SEM images of (a) Pd@In_2O_3 catalyst derived from Pd-TCPP@MIL-68(In) at TCPP(Pd) loading content of 2.8 wt%, (d-f) IWI-Pd-In_2O_3 catalyst prepared from using Pd^{2+}@MIL-68(In) as a precursor.

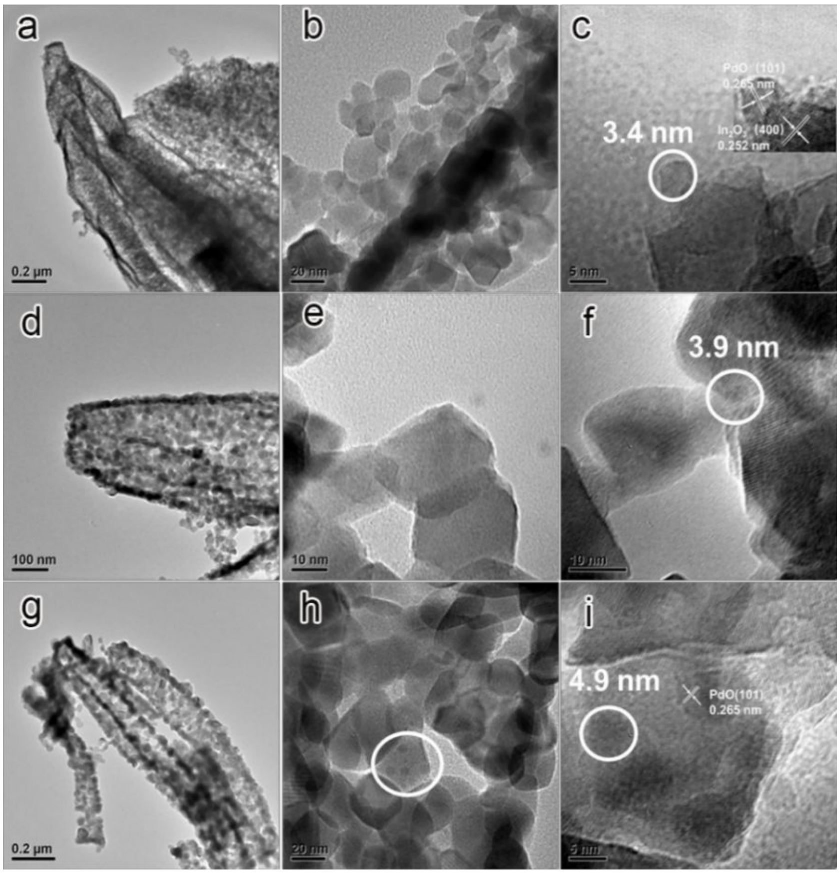

Figure S5. Representative TEM images at different magnifications of Pd@In_2O_3-x catalysts with different calcination temperatures. (a-c) 600 °C, (d-f) 700 °C, and (g-i) 800 °C.

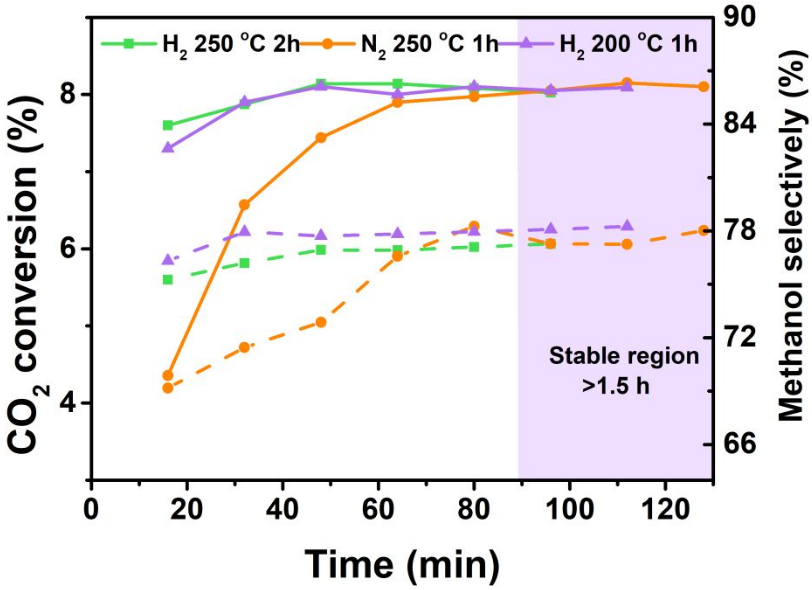

Figure S6. The comparisons of CO_2 conversion and methanol selectively over the Pd@In_2O_3 catalyst under different pretreatment conditions (temperature, time, and atmospheres).

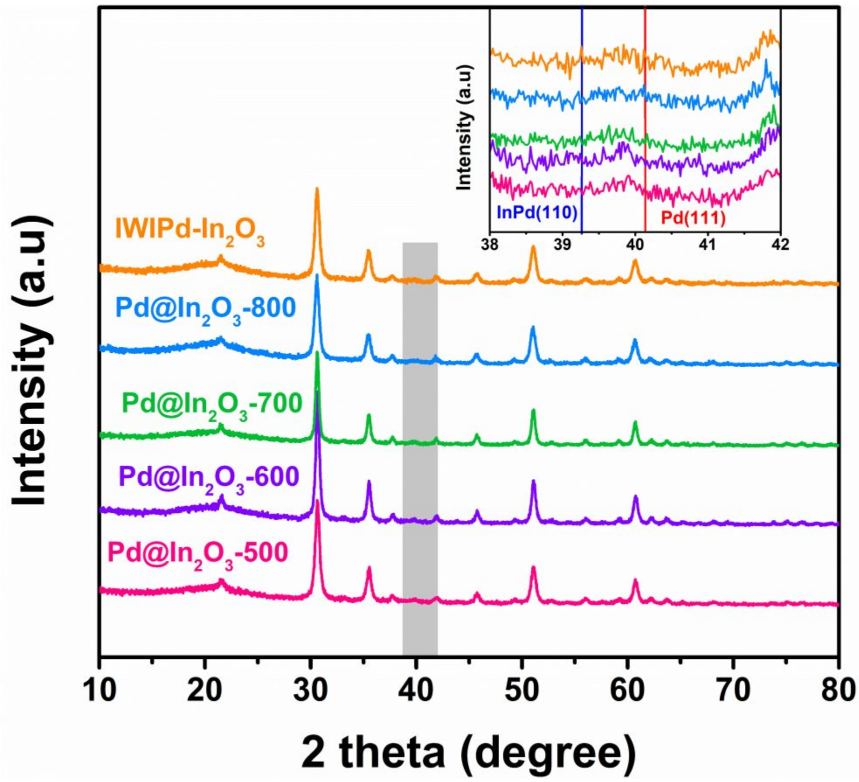

Figure S7. XRD patterns of the spent Pd/In_2O_3 and IWI-Pd/In_2O_3 catalysts.

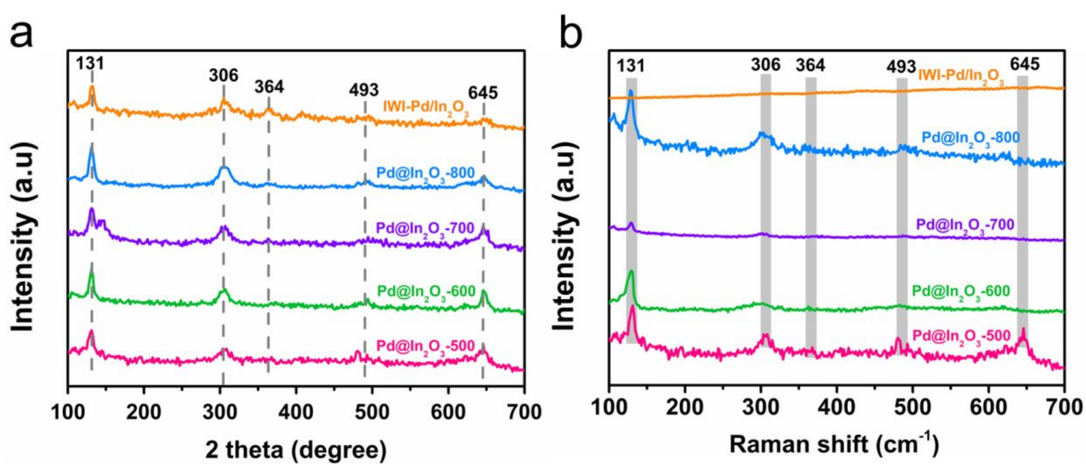

Figure S8. (a) Raman spectra of the calcination catalyst and (b) Raman spectra of the spent catalyst.

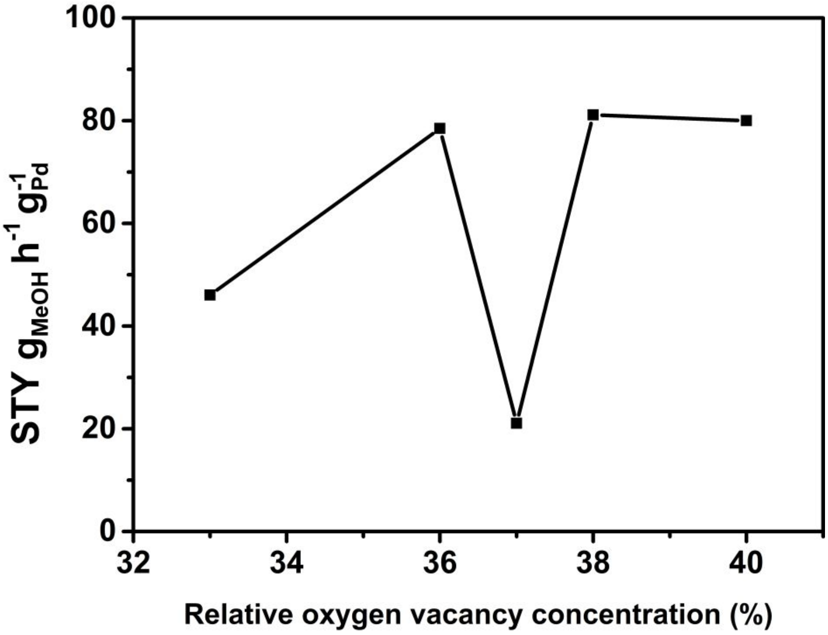

Figure S9. The space-time yield (STY) of methanol as a function of the relative concentration of oxygen vacancy.

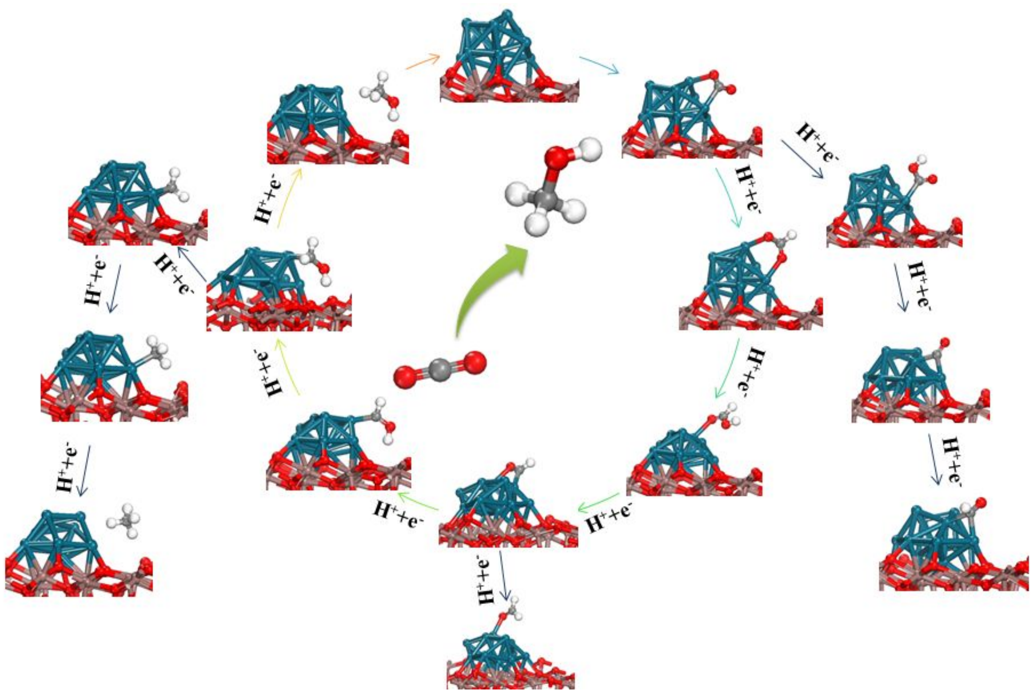

Figure S10. Structure diagrams of the important intermediates in the catalytic CO_2 hydrogenation on the surface of the Pd/In_2O_3 catalyst. Color codes: white, H atoms; red, O atoms; brown, In atoms; cyan, Pd atoms.

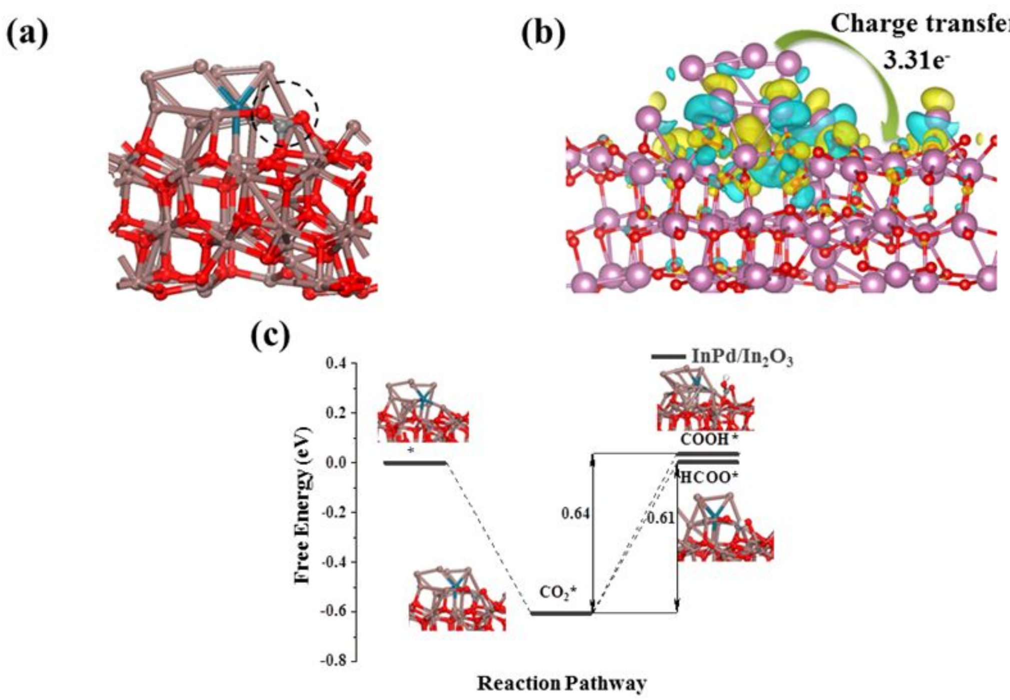

Figure S11. (a) CO_2 adsorption structure, (b) charge transfer, and (c) the catalytic pathway on the InPd/In_2O_3 catalyst.

Table S1 Synthetic parameters and the corresponding average length and width of the prepared MIL-68(In) composites.

Sample	TCPP(Pd) (mg)	H_2BDC (mg)	$In(NO_3)_3$ (mg)	DMF (mL)	Length (um)	Width (um)	S_{BET} m^2/g	V_{pore} cm^3/g
TCPP(Pd)@MIL-68(In)	0	200	408.2	5.0	4.6±0.5	1.0±0.2	846	0.68
	10	200	408.2	5.0	6.0±1.2	1.0±0.2	701.5	0.46
	15	200	408.2	5.0	6.9±1.0	1.4±0.2	675.9	0.20
	20	200	408.2	5.0	8.1±1.5	1.4±0.5	156.6	0.11
	25	200	408.2	5.0	8.4±1.5	1.4±0.4	60.5	0.08
	30	200	408.2	5.0	8.5±1.5	1.4±0.6	n.a.	n.a.

Table S2 Comparison of CO_2 hydrogenation to methanol over different catalysts.

Catalyst	T [K]	P [MPa]	GHSV (mL g_{cat}^{-1} h^{-1})	S_{MeOH} (%)	STY_{MeOH} (g_{MeOH} h^{-1} g_x^{-1})	Ref.
PdIn-In_2O_3/SiO_2[a]	573	5.0	63000	24	3.6	1
Pd/In_2O_3-CP[b]	553	5.0	24000	75	81.3	2
Pd/In_2O_3/SBA-15	543	5.0	15000	83.9	3.5	3
Pd-P/In_2O_3[c]	573	5.0	21000	71	97.8	4
Pt/In_2O_3	573	5.0	21000	54	52.6	5
Au/In_2O_3	573	5.0	21000	67.8	23.2	6
Ir/In_2O_3	573	5.0	21000	70	7.65	7
Pd/CeO_2	513	3.0	6000	47.7	1.16	8
Pd-ZnO@ZIF-8	563	4.5	19200	78	19.8	9
h-In_2O_3/Pd[d]	568	3.0	24000	74	41.9	10
Pd@In_2O_3-500	568	3.0	19200	74	79.2	our work
Pd@In_2O_3-600	568	3.0	19200	81	81.1	our work

Notes: S_{MeOH} represents the selectivity of methanol, and STY_{MeOH} represents the space-time yield of methanol-based on the weight of the supported noble metals such as Pd, Pt, Au, and Ir, etc.

[a]: Both PdIn alloy and In_2O_3 were supported on SiO_2.

[b]: Pd-In_2O_3 catalyst was synthesized by co-precipitated (CP).

[c]: Pd was supported on In_2O_3 by using the peptide as a modifier (Pd-P).

[d]: Pd nanoparticles were supported on hollow-tube structure In_2O_3 (*h*-In_2O_3).

Table S3 Comparision of the M/In_2O_3 catalysts with different noble metals loading contents on In_2O_3 support for CO_2 hydrogenation.

Catalyst	Noble metal loading (wt%)	Temp. (K)	Pressure (MPa)	H_2/CO_2	Catalytic performance		Ref.
					CO_2 conv. (%)	Methanol selec. (%)	
Pd/In_2O_3	0.93	573	5.0	4	20	71	[4]
Pd/In_2O_3	0.75	553	5.0	4	9.2	78	[2]
Pd/In_2O_3	1.36	568	3.0	3	10.5	72.4	[10]
Pd/In_2O_3	5.0	523	3.	3	1.9	72	[10]
Pt/In_2O_3	1.07	573	5.0	4	17.3	54	[10]
Au/In_2O_3	2.0	573	5.0	4	11.7	67.8	[10]
Ir/In_2O_3	1.0	573	5.0	4	11.6	70	[10]
Pd@In_2O_3	0.5	568	3.0	3	8.1	81.1	our work

References

1. Snider, J. L.; Streibel, V.; Hubert, M. A.; Choksi, T. S.; Valle, E.; Upham, D. C.; Schumann, J.; Duyar, M. S.; Gallo, A.; Abild-Pedersen, F.; Jaramillo, T. F., Revealing the Synergy between Oxide and Alloy Phases on the Performance of Bimetallic In–Pd Catalysts for CO_2 Hydrogenation to Methanol. *ACS Catal.* **2019,** *9* (4), 3399-3412.

2. Frei, M. S.; Mondelli, C.; Garcia-Muelas, R.; Kley, K. S.; Puertolas, B.; Lopez, N.; Safonova, O. V.; Stewart, J. A.; Curulla Ferre, D.; Perez-Ramirez, J., Atomic-scale engineering of indium oxide promotion by palladium for methanol production via CO_2 hydrogenation. *Nat. Commun.* **2019,** *10* (1), 3377.

3. Jiang, H.; Lin, J.; Wu, X.; Wang, W.; Chen, Y.; Zhang, M., Efficient hydrogenation of CO_2 to methanol over Pd/In_2O_3/SBA-15 catalysts. *Journal of CO_2 Utilization* **2020,** *36*, 33-39.

4. Rui, N.; Wang, Z.; Sun, K.; Ye, J.; Ge, Q.; Liu, C.-j., CO_2 hydrogenation to methanol over Pd/In_2O_3: effects of Pd and oxygen vacancy. *Appl. Catal. B* **2017,** *218*, 488-497.

5. Sun, K.; Rui, N.; Zhang, Z.; Sun, Z.; Ge, Q.; Liu, C.-J., A highly active Pt/In_2O_3 catalyst for CO_2 hydrogenation to methanol with enhanced stability. *Green Chem.* **2020,** *22* (15), 5059-5066.

6. Rui, N.; Zhang, F.; Sun, K.; Liu, Z.; Xu, W.; Stavitski, E.; Senanayake, S. D.; Rodriguez, J. A.; Liu, C.-J., Hydrogenation of CO_2 to Methanol on a $Au^{\delta+}$–In_2O_{3-x} Catalyst. *ACS Catal.* **2020,** *10* (19), 11307-11317.

7. Shen, C.; Sun, K.; Zhang, Z.; Rui, N.; Jia, X.; Mei, D.; Liu, C.-j., Highly Active Ir/In_2O_3 Catalysts for Selective Hydrogenation of CO_2 to Methanol: Experimental and Theoretical Studies. *ACS Catal.* **2021,** *11* (7), 4036-4046.

8. Jiang, F.; Wang, S.; Liu, B.; Liu, J.; Wang, L.; Xiao, Y.; Xu, Y.; Liu, X., Insights into the Influence of CeO_2 Crystal Facet on CO_2 Hydrogenation to Methanol over Pd/CeO_2 Catalysts. *ACS Catal.* **2020,** *10* (19), 11493-11509.

9. Li, X.; Liu, G.; Xu, D.; Hong, X.; Edman Tsang, S. C., Confinement of subnanometric PdZn at a defect enriched ZnO/ZIF-8 interface for efficient and selective CO_2 hydrogenation to methanol. *J. Mater. Chem. A* **2019,** *7* (41), 23878-23885.

10. Cai, Z.; Dai, J.; Li, W.; Tan, K. B.; Huang, Z.; Zhan, G.; Huang, J.; Li, Q., Pd Supported on MIL-68(In)-Derived In_2O_3 Nanotubes as Superior Catalysts to Boost CO_2 Hydrogenation to Methanol. *ACS Catal.* **2020,** *10* (22), 13275-13289.

11 Zhu, J.; Cannizzaro, F.; Liu, L.; Zhang, H.; Kosinov, N.; Filot, I. A. W.; Rabeah, J.; Bruckner, A.; Hensen, E. J. M., Ni-In Synergy in CO_2 Hydrogenation to Methanol. *ACS Catal* **2021,** *11* (18), 11371-11384.